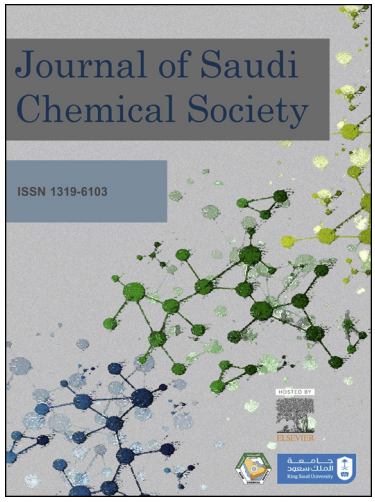

Original article

Fermented juices as reducing and capping agents for the biosynthesis of size-defined spherical gold nanoparticles

Anna Dzimitrowicz, Piotr Jamroz, George C. diCenzo, Wojciech Gil, Wojciech Bojszczak, Agata Motyka, Dorota Pogoda, Pawel Pohl

PII: S1319-6103(17)30147-3
DOI: https://doi.org/10.1016/j.jscs.2017.12.008
Reference: JSCS 933

To appear in: *Journal of Saudi Chemical Society*

Received Date: 22 August 2017
Revised Date: 13 December 2017
Accepted Date: 15 December 2017

Please cite this article as: A. Dzimitrowicz, P. Jamroz, G.C. diCenzo, W. Gil, W. Bojszczak, A. Motyka, D. Pogoda, P. Pohl, Fermented juices as reducing and capping agents for the biosynthesis of size-defined spherical gold nanoparticles, *Journal of Saudi Chemical Society* (2017), doi: https://doi.org/10.1016/j.jscs.2017.12.008

Title: Fermented juices as reducing and capping agents for the biosynthesis of size-defined spherical gold nanoparticles

Authors: Anna Dzimitrowicz[a*], Piotr Jamroz[a], George C diCenzo[b], Wojciech Gil[c], Wojciech Bojszczak[a], Agata Motyka[d], Dorota Pogoda[e], Pawel Pohl[a]

Affiliations: [a]*Wroclaw University of Science and Technology, Faculty of Chemistry, Department of Analytical Chemistry and Chemical Metallurgy, Wybrzeze Wyspianskiego 27, 50-370 Wroclaw, Poland*

[b]*University of Florence, Department of Biology, via Madonna del Piano 6, 50-143 Sesto Fiorentino, Italy*

[c]*University of Wroclaw, Faculty of Chemistry, F. Joliot-Curie 14, 50-383 Wroclaw, Poland*

[d]*University of Gdansk, Department of Biotechnology, Laboratory of Plant Protection and Biotechnology, Antoniego Abrahama 58, 80-307 Gdansk, Poland*

[e]*Wroclaw University of Science and Technology, Faculty of Chemistry, Institute of Inorganic and Structural Chemistry, Wybrzeze Wyspianskiego 27, 50-370 Wroclaw, Poland*

*Corresponding author. E-mail address: anna.dzimitrowicz@pwr.edu.pl

ABSTRACT

Gold nanoparticles (AuNPs) are of scientific and industrial significance; however, traditional synthesis methods employ toxic compounds. Hence, non-toxic and environmentally friendly AuNPs synthesis methods are of special interest. Here, AuNPs were produced using four solutions of fermented grape juices. UV/Vis absorption spectrophotometry and transmission electron microscopy indicated that AuNPs synthesized with a solution based on semi-sweet red grapes were mostly spherical with narrow size distribution (average diameter of 82.1±36.2 nm). AuNPs of similar spherical morphology but smaller size were obtained using a solution based on semi-dry red grapes (57.1±16.4 nm). A large variety of AuNPs shapes and broader size distribution were produced when solutions based on semi-sweet or dry white grapes were applied. In this case, the average sizes of the AuNPs were 271.6±130.2 nm and 76.0±47.2 nm, respectively. Using energy dispersive X-ray spectroscopy, Au, C, and O were detected, confirming formation of biogenic AuNPs in all cases. Mie theory calculations for AuNPs synthesized with the aid of solutions based on red grapes suggest that their optical properties are different and best suited for distinct downstream applications. Attenuated total reflectance Fourier transform infrared spectroscopy, the Folin-Ciocalteu assay, and the Bertrand's method were used to examine bioactive compounds present in the solutions applied for synthesis. Phenolics, and to a lesser extent reducing sugars, were identified as likely playing a significant role in reduction and stabilization of the AuNPs. These results display the great potential of these solutions for the green synthesis of size defined AuNPs, and illustrate that different grape varieties may be used to obtain AuNPs with unique properties.

Keywords: nanostructures; bioreduction process; phenolics; reducing sugars; Mie scattering

1. INTRODUCTION

Gold nanoparticles (AuNPs), being pure metallic Au structures in which at least one dimension is less than 100 nm, have found applications in diverse scientific and industrial fields. This includes medicine and diagnostics [1-6], biosensoring [7-9], and catalysis [10-12]. AuNPs can contain oxidized centers [13], which during gold catalysis can undergo *in situ* reduction by the substrate [14]. As a result, there is high demand for production of large amounts of their colloidal suspensions, which typically involves reduction of the Au(III) ions to metallic Au [15], however, this often, but not always, involves hazardous reducing compounds. Therefore, recent research has been focused on development of environmentally friendly, rapid, and low-cost methods for synthesis of stable in time Au nanodispersions with defined optical properties and morphology. Accordingly, one of such approaches to preparation of the colloidal suspensions of biocompatible AuNPs is the use naturally occurring reducing agents originating from plant leaves [16-20], fruit extracts [21], or purified essential oils [17, 22]. These mixtures of bioactive compounds are directly involved in bioreduction of the Au(III) ions (see examples in Table 1), negating the need of toxic compounds application. A poorly explored class of biological mixtures, in regards to AuNPs synthesis, is natural, ubiquitous, and inexpensive food products, which constituents may facilitate reduction of the Au(III) ions to AuNPs. To the best of our knowledge, only honeys [23], mijiu [24], and fruit juices [25] have been used so far for this purpose (Table 1).

Utilization of fermented grape juices in the biosynthesis of AuNPs is especially intriguing as there is a large variety in the type and origin of grapes that may allow for synthesis of AuNPs with equally diverse sizes and shapes. There are over 1,000 grapevine cultivars (*Vitis vinifera* L.) used in production of such solutions, each selected to achieve distinct properties such as differences in sugar content [26]. The chemical composition of each solution is further influenced by geographical origin, harvest time, and the production

process [27]. These solutions contain numerous organic substances [28] that may contribute to reduction of the Au(III) ions to AuNPs as well as to promote their subsequent stability. Phenolics, e.g. hydroxycinnamates, benzoic acids, stilbenes, flavonan-3-ols, flavonols, and anthocyanins, which are responsible for antioxidant properties of these solutions [29], are of particular interest in reference to AuNPs synthesis because they can readily be oxidized, contributing to the bioreduction process [16]. The concentration of phenolics can differ dramatically, particularly between the use of white grapes, where only the juice is used, compared to the use of red grapes, where the production process involves the juice as well as the solids, skins, and seeds that contain most of the phenolic substances [29, 30]. The average total amount of phenolic compounds is ~ 210 and 1,700 mg L^{-1} for the use of white and red grapes, respectively [29].

The objective of the present work was to examine whether such solutions could be employed as alternative reducing and capping agents for green synthesis of AuNPs, and to verify how the choice of variety influences the properties of the resulting nanoparticles. Four types of solutions (based on semi-sweet red, sweet-dry red, semi-sweet white, and dry white grapes) were used and their ability to serve as reducing and stabilizing agents was tested. Optical properties, size, shape, and the elemental composition of biosynthesized AuNPs were assessed by UV/Vis absorption spectrophotometry, transmission electron microscopy (TEM), and energy dispersive X-ray spectroscopy (EDX). In addition, scattering and absorption properties of biosynthesized AuNPs were estimated *in silico*. Attenuated total reflectance Fourier transform infrared spectroscopy (ATR FT-IR) was used to study which bioactive compounds present in the examined solutions might be responsible for reduction of the Au(III) ions and stabilization of resulting AuNPs. Additionally, determination of the total concentration of phenolics and reducing sugars in the solutions was carried out using the Folin-Ciocalteu (F-C) assay and the Bertrand's method, respectively.

2. MATERIALS AND METHODS

2.1. Reagents and solutions

Chloroauric acid tetrahydrate ($HAuCl_4 \times 4H_2O$) was purchased from Avantor Performance Materials (Gliwice, Poland). Four types of commercially available fermented grape solutions, i.e. semi-sweet red (grape variety – Blaufrankisch; origin – Hungary; production year – 2014), semi-dry red (grape variety – Carmenere; origin – Chile; production year – 2014), semi-sweet white (grape variety – Souvignion; origin – Moldova; production year – 2015), and dry white (grape variety – Chenin blanc; origin – South Africa; production year – 2015), were obtained from a local market. Working solutions were obtained by diluting the commercial solutions to a concentration of 5% (v/v) with re-distilled water.

2.2. Green biosynthesis of AuNPs

To produce the colloidal suspensions of AuNPs, a bulky $HAuCl_4$ solution was added to the 5% (v/v) fermented grape juice solutions to obtain a final concentration of the Au(III) ions at 25, 50, or 100 mg L^{-1}. To find the optimal conditions for the biosynthesis of AuNPs, three concentrations of fermented juice solutions, *i.e.* 5, 10, and 15% (v/v), and three final concentrations of Au(III) ions (25, 50, or 100 mg L^{-1}) were analyzed. As a circa the symmetrical localized surface plasmon resonance absorption band was detected only when using the lowest concentration (i.e. 5% [v/v]), it was chosen that the 5% solutions would be used in subsequent experiments The resulting reaction mixtures were incubated at room temperature for 120 s. The obtained Au nanodispersions were subsequently kept at 4 ºC in dark until further characterization.

2.3. Characterization of AuNPs

UV/Vis absorption spectrophotometry was used to determine the optical properties of the resulting colloidal AuNPs suspensions. An Analytic Jena AG (Jena, Germany) UV/Vis double-beam spectrophotometer, model Specord 210 Plus was used. The absorption spectra of the reaction mixtures in the range of 400-1000 nm were acquired 24 h after synthesis. A scanning speed of 20 nm s^{-1} and a step of 0.1 nm were used. The spectrometer was zeroed using re-distilled water to obtain baseline readings. In order to assess the morphology of the nanostructures, the AuNPs were purified from the solutions by centrifugation at 14,500 *g* for 90 min in a MPW-55 centrifuge (MPW Medical Instruments, Warsaw, Poland). The supernatant was discarded, and the pellet was washed three times with re-distilled water. Then, the pellet was re-dispersed in re-distilled water and collected for further analyses.

To evaluate size, shape, and the elemental composition of biosynthesized AuNPs, a FEI Tecnai G^2 20 X-TWIN transmission electron microscope TEM instrument (FEI, Hillsboro, USA), equipped with an EDX system (Oxford Aztec Energy), was applied. The samples were prepared by placing 100 µL aliquots of the colloidal AuNPs suspensions onto Cu mesh grids (CF 400 Cu-UL, Electron Microscopy Sciences, Hatfield, PA, USA), which were then left to dry at room temperature. The average sizes of AuNPs were calculated on the basis of 30 measurements of diameter of individual spherical and polygonal AuNPs, or their height in case of triangular structures, imagined with TEM.

2.4. ATR FT-IR analysis of the solutions

ATR FT-IR was used to identify the organic compounds present in studied solutions and likely being responsible for the AuNPs biosynthesis. The ATR FT-IR spectra of the 5% solutions were acquired at wavenumbers changed from 4000 to 400 cm^{-1} with resolution of 4 cm^{-1}. A Bruker (Bremen, Germany) Vertex 70v FT-IR spectrophotometer with a diamond

ATR cell was used for that purpose. All measurements were performed in vacuum conditions.

2.5. Quantitative analyses of phenolics and reducing sugars

To determine the concentration of phenolic compounds in studied solutions used for the biosynthesis of AuNPs, a spectrophotometric method based on the Folin-Ciocalteu assay was applied as described before [31]. Half a mL of the examined 5% (v/v) solutions were mixed with 2.5 mL of a 10-fold diluted solution of the Folin-Ciocalteu reagent (Sigma-Aldrich, Poznan, Poland) and incubated at room temperature for 2 min. Next, 2 mL of a 7.5% (m/v) Na_2CO_3 solution were added to these mixtures and incubated for 15 min at 50 ºC. Finally, they were placed into a water-ice bath for 4 min. The absorbance of the phosphotungstic-phosphomolybdenum complex formed in the resulting reaction mixtures was measured at 765 nm. A calibration curve for the gallic acid (GA) standard solutions was prepared within the range of 30-150 mg L^{-1} following the same procedure. The final results were expressed as mg of the GA equivalents per L of the examined undiluted solution.

The concentration of reducing sugars before and after addition of the Au(III) ions was determined by applying the Bertrand's method, which is based on the amount of the Cu(II) ions reduced to Cu_2O [32]. Briefly, 20 mL of the examined 5% solutions were mixed with 20 mL of Bertrand I solution ($CuSO_4$) and 20 mL of a Bertrand II solution (mixture of NaOH and $C_4H_4KNaO_6$). The resulting mixtures were boiled for 3 min and, after cooling, the Cu_2O precipitates formed were carefully washed with hot water by decanting through a glass Gootch crucible G-1. Next, the precipitates were dissolved using 20 mL of a Bertrand III solution (mixture of $Fe_2(SO_4)_3$ and H_2SO_4). Finally, the resulting solutions were titrated using a 0.02 mol L^{-1} $KMnO_4$ standard solution until stable slight pink color was achieved. One mL of this titrating solution corresponded to 6.357 mg of the reduced Cu(II) ions. The amount of

reducing sugars (in mg) in the examined 5% solutions was calculated on the basis of the amount of the reduced Cu ions (in mg) in the following way: reducing sugars (in mg) = 0.546 × reduced Cu (in mg).

2.6. Mie theory calculations

Extinction and scattering efficiencies were calculated in Python using a published Python script [33], based on an earlier Matlab script [34]. Absorption efficiencies were calculated as the difference between the extinction and scattering efficiencies at each wavelength. Mie calculations were performed using Python 2.7.10, with Scipy 0.15.1 and Numpy 1.9.2. A reflective index of 1.33 (water at 20 °C) was used, and diameters of AuNPs synthesized using solutions based on the semi-sweet red and semi-dry red grapes were as determined using TEM.

2.7. Yield of the AuNPs biosynthesis

The efficiency of the AuNPs synthesis processes using 25 mg L^{-1} of Au(III) as a precursor concentration was assessed using flame atomic absorption spectrometry (FAAS). AuNPs (purified from the reaction mixture by centrifugation as described above) were digested in 1.5 mL of aqua regia. After this, a PerkinElmer 1100B FAAS instrument (Waltham, USA) was applied to estimate the amount of Au converted into AuNPs in each of the reaction.

3. RESULTS AND DISCUSSION

3.1. Optical properties of the Au nanodispersions

Four solutions based on fermented grape juices were used for the production of AuNPs, each based on a different grape variety: Solution I (semi-sweet red), Solution II

(semi-dry red), Solution III (semi-sweet white), and Solution IV (dry white). The production of colloidal AuNPs suspensions is associated with a change in the color of the solution [35]. Following incubation with the Au(III) ions, Solutions I and II changed color from pale pink to ruby red, while Solutions III and IV changed color from pale yellow to bluish. To further examine AuNPs formed in the resulting reaction mixtures, their optical properties were determined with UV/Vis absorption spectrophotometry. Intense localized surface plasmon resonance (LSPR) absorption bands, particularly for Solutions I and II, were observed (Fig. 1), which confirmed the production of the colloidal AuNPs suspensions. In the cases of Solutions I and II, the LSPR absorption bands were quite symmetrical, indicating production of uniform in size spherical AuNPs. The position of the wavelength at the maximum of the LSPR band (λ_{max}) was located at 557.0 nm and 550.6 nm for Solution I and Solution II, respectively. By contrast, for Solutions III and IV, the LSPR absorption bands were less intensive but still symmetrical indicating rather uniform size distribution. The position of the λ_{max} of these LSPR absorption bands was 553.6 nm and 558.2 nm, respectively, for AuNPs synthesized with Solution III and Solution IV. In addition, weak absorption bands, likely attributed to the longitudinal plasmon resonance, were identified in the colloidal AuNPs suspensions produced with the aid of Solutions III and IV, which suggested production of non-spherical Au nanostructures [36, 37].

The effect of the concentration of the Au(III) ions on the optical properties of the resultant AuNPs was also examined. Figure 2 shows the relation between the absorbance of the λ_{max} of the LSPR absorption band and the initial concentration of the Au(III) ions. Except for Solution IV, an increase in the concentration of the Au(III) ions resulted in a gradual increase in the absorbance of the LSPR band, which indicated greater AuNPs production yields in these conditions [36]. At all studied concentrations of the Au(III) ions, higher

absorbance values of the LSPR absorption band were recorded for the reaction mixtures involving Solutions I and II than those with Solutions III and IV.

Commonly, the λ_{max} of the LSPR band is red-shifted as the concentration of the Au(III) ions increases [16], which, according to the Mie scattering theory, is indicative of larger AuNPs production [38]. In this work, a shift in position of the λ_{max} of the LSPR band toward longer wavelengths was observed only for the reaction mixtures with Solutions III and IV. Surprisingly, the position of the LSPR absorption band was blue-shifted as the concentration of the Au(III) ions was increased in the reaction mixtures with Solutions I and II. In all cases, no linear correlation between the concentration of the Au(III) ions and position of the LSPR absorption band was observed.

3.2. Effectiveness of the AuNPs biosynthesis

The less intensive LSPR bands in the cases of Solutions III and IV suggested that the AuNPs yield using these solutions were lower than when using Solutions I or II. Therefore, the FAAS technique was used to examine the effectiveness of the AuNPs synthesis using each of the four solutions and 25 mg L^{-1} of the Au(III) precursor. It was observed that 63% and 60% of the Au ions were incorporated into AuNPs when using Solutions I and II, respectively. Somewhat lower values were observed with Solutions III and IV, 51% and 57%, respectively. These results confirmed that the yield with Solutions I and II was higher than with Solutions III and IV.

3.3. Characterization of the AuNPs morphology

Further characterization of the size and shape of the biosynthesized AuNPs was performed using TEM. As shown in Figures 3A-3C, AuNPs obtained with Solution I were mostly spherical and uniform in size. Their average diameter was 82.1±36.2 nm (see Fig.

4A). It should be noted, however, that most of biosynthesized AuNPs consisted of aggregated grains with average diameter of 21.4±8.6 nm. AuNPs achieved using Solution II were spherical as well (Figs. 3E-3G) but with a more narrow size distribution (Fig. 4B, diameter of 57.1±16.4 nm). In this case, agglomeration of smaller AuNPs (average diameter of 18.9±5.0 nm) was also observed.

In contrast, a high variety of shapes of biosynthesized AuNPs was observed when Solutions II or IV were applied. For Solution III, only polygon-shaped AuNPs were found (Figs. 3I-3K). The resulting AuNPs had quite a broad size distribution with an average size of 270.6±130.2 nm (Fig. 4C). Using Solution IV, a variety of shapes of Au nanostructures was seen, including spherical (85%), triangular (10%) and hexagonal (5%) (Figs. 3M-3O). Average size of these AuNPs was smaller than those obtained with Solution II, i.e. 76.0±47.2 nm (Fig. 4D). Unlike AuNPs produced with Solutions I or II, AuNPs synthesized with Solutions III or IV were sufficiently well-dispersed and only slightly aggregated. It is not clear why a variety of AuNPs shapes were detected when using Solutions III or IV. However, as described below, a correlation was detected between the characteristics of the AuNPs and the concentration of phenolics in the solutions. Thus, it may be that the lower concentration of these potential reducing and capping agents contributed to the shape differences.

EDX analyses were conducted to determine the elemental composition of the biosynthesized AuNPs. In all four cases, intense peaks of Au were identified in the EDX spectra, confirming that the structures observed with TEM were indeed AuNPs (Figs. 3D, 3H, 3L, 3P). Additionally, peak representing presence of O, C, and Cu (from the Cu grids) were found in all analyzed samples.

Overall, the optical and morphological analyses confirmed that all four of the tested solutions could mediated the synthesis of AuNPs. Additionally, the data were consistent with

solutions based on red grapes being better suited for the synthesis of size-defined, spherical nanoparticles.

3.4. Mie theory calculations for the biosynthesized AuNPs

Size and shape of AuNPs strongly influence their downstream applications. For example, AuNPs of 40 nm in diameter are often employed in laser photothermal cancer therapy [39, 40], while surface enhanced Raman spectroscopy (SERS) is the most efficient when AuNPs of ~50 nm in diameter are applied [41]. In general, AuNPs with high absorption efficiency but low scattering efficiency are valuable in photothermal therapies, whereas AuNPs with high scattering efficiency are of potential use in light-scattering microscopy [39]. Therefore, Mie theory calculations, carried out in Python as described previously [33], were used to predict absorption and scattering properties of the biosynthesized AuNPs in a water environment. As the calculations assume a spherical shape of the AuNPs, calculations were made only for AuNPs produced with Solutions I or II. AuNPs synthesized with the Solution II (with average diameter of 57.1 nm) were estimated to have an absorption efficiency ~4.5-fold higher than the scattering efficiency, with maximums at 531 and 541 nm, respectively (Fig. 5). By contrast, AuNPs synthesized with Solution I (with average diameter of 82.1 nm) had an absorption efficiency only ~1.3-fold higher than the scattering efficiency, with maximums at 542 and 562 nm, respectively (Fig. 5). Additionally, the intensity of the per particle extinction of the 82.1 nm AuNPs was estimated to be approximately 1.4-fold stronger than of 57.1 nm AuNPs, with maximums at 550 and 533 nm, respectively. The predicted differences in the optical properties of the AuNPs synthesized with these two solutions suggest that these nanomaterials may be optimally employed in different downstream applications, such as SERS or light-scattering microscopy.

3.5. Chemical composition of solutions used for the AuNPs synthesis

To identify chemical compounds that might be responsible for AuNPs biosynthesis, ATR FT-IR spectroscopy was used. The ATR FT-IR spectra profiles of the examined solutions were quite similar, suggesting that the same classes of organic compounds were present in each solution (Fig. 6). The most intense absorption bands in the FT-IR spectra of all solutions were identified in the range of 1503-1687 cm^{-1} and 2975-3650 cm^{-1}. These bands were associated with stretching vibrations ν of the OH group from water and ethanol [42, 43]. Presence of ethanol was additionally confirmed by the very strong absorption band with maximum at 1042 cm^{-1}, caused by stretching vibrations ν of the C-O bond [44]. Based on the intensities of these bands, it was presumed that the ethanol concentration was the highest in Solution I and the lowest in Solution IV. The presence of high amounts of ethanol contributed to the efficient dispersion of the AuNPs, as was previously described by Lu et al. for magnetic nanoparticles [45].

Symmetrical and asymmetrical stretching vibrations ν of the -C=O group were identified on the basis of the absorption bands with maximums at 1723 cm^{-1}, 1615 cm^{-1}, and 1410 cm^{-1} [46]. These IR bands suggested occurrence of carboxylic acids, e.g. tartrate, malate, succinic, and acetic acids [47-50], and phenolics such as cinnamic acids, myricetin, and quercetin [50, 51]. The absorption band in the region of 1393-1400 cm^{-1} was also found and related to bending vibrations of the -O-H group in carboxylic acids [50]. In addition, absorption bands with maximums at 1610 cm^{-1} and 1518 cm^{-1} were observed and possibly linked to stretching vibrations ν of the C=C bonds in the molecules with aromatic rings in their structure, particularly phenolic compounds [50]. Based on the spectra, it was presumed that Solution IV contained the most organic acids, while the amount of these species in Solution I was the lowest.

The absorption bands of simple carbohydrates were observed in the range of 1200-950 cm^{-1}. They were allocated to stretching vibrations ν of the C-C and C-O bonds [53]. Particularly, the intense IR band with maximum around 1074 cm^{-1} was assigned to stretching vibrations ν of the C-O-C bond in cyclic alcohol ethers present in D-(-)-fructose [54]. The absorption band at 555 cm^{-1} was associated with deforming vibrations δ of the C-C-C, C-C-O, C-O bonds as well as skeleton vibration characteristic for D-(+)-glucose [54]. It appeared that the highest amount of D-(-)-fructose was present in Solution II.

Overall, ATR FT-IR analysis pointed out that the main classes of compounds present in the examined solutions where rather similar; however, their concentrations and likely the specific molecules within each class differed between solutions. These differences in the composition between solutions likely resulted in differences in their reducing and stabilizing properties, leading to the observed differences in the characteristics of the biosynthesized AuNPs.

3.6. Total contents of phenolics and reducing sugars in the solutions

Phenolics and reducing sugars present in plant extracts seem to play a crucial role in the biosynthesis of AuNPs [16]. Therefore, the total concentration of phenolic compounds and reducing sugars in Solutions I to IV before and after addition of the Au(III) ions was determined. In all cases, it was established that addition of the Au(III) ions to the solutions resulted in a decrease in the total concentration of these organic compounds (see Tables 2 and 3). This was suggestive of their oxidation during reduction of the Au(III) ions to AuNPs.

However, no correlation between the initial concentration of reducing sugars and the optical properties of the obtained AuNPs, as determined by the λ_{max} of the LSPR band, or size, as determined using TEM, was established (Table 3). A separate study suggested that reducing sugars derived from natural products can be new functional molecules for the green

synthesis of nanostructures and nanomaterials [55]. They themselves and/or their oxidized products are environmentally friendly, while the resulting nanostructures are biocompatible. Thus, while reducing sugars were likely involved in the reduction process in this study as well, the lack of correlation suggests they were not the major factor responsible for the AuNPs characteristics. On the other hand, it was found that Solutions I and II contained at least five times more phenolic compounds than Solutions III and IV (Table 2). Moreover, AuNPs biosynthesized with Solutions I and II were spherical and smaller in size than the AuNPs of different shapes produced through the use of Solutions III and IV (Figs. 3 and 4). Phenolics are a group of plant secondary metabolites that have commonly been reported to be responsible for the bioreduction of metals ions to the nanometric size structures (see for example, [16, 29, 56-58]). The observed relationship between the total concentration of phenolic compounds in the solutions and the size of biosynthesized AuNPs in the present work may suggest that phenolics can be one of the main decisive factors that determines the size of the biosynthesized AuNPs. This may be accomplished by acting as capping agents that prevent uncontrolled growth of the Au nanostructures. The content of phenolic compounds may have also influenced the yield of AuNPs obtained by green synthesis.

4. CONCLUSIONS

A novel single-phase bioreduction process for the production of AuNPs in aqueous fermented grape juice solutions is proposed. Homogeneous and spherical AuNPs can be fabricated using solutions prepared from red grapes, while the use of solutions based on white grapes tends to produce AuNPs of various shapes. Phenolic compounds, and to a lesser extent reducing sugars, appear to play a critical role in reduction of the Au(III) ions as well as capping and stabilization of biosynthesized AuNPs in the reaction mixtures. Both of these naturally occurring groups of compounds and/or their oxidized products seem to be

environmentally friendly; hence, the resulting organically-capped AuNPs can be used for a wide range of biomedical and bioenvironmental applications. This process of green synthesis of AuNPs is simple, cost-effective, and provides an ability to control the size, shape, and stability of the AuNPs. Additional studies are needed to find the relationship between the concentration of total or individual phenolic compounds and sugars present in the solutions and the size and shape of the biosynthesized AuNPs. Nevertheless, the described procedure can open up new possibilities for alternative, inexpensive, and large-scale production of AuNPs. Finally, it can be hypothesized that by testing a greater number of grape varieties a set of grapes will be identified that allow for size-defined synthesis of AuNPs.

ABBREVIATIONS

ATR FT-IR: attenuated total reflection Furrier transformation-infrared spectroscopy

AuNPs: gold nanoparticles

EDX: X-ray energy dispersive spectroscopy

FC assay: Folin-Ciocalteu assay

GA: gallic acid

LSPR: localized surface plasmon resonance

TEM: transmission electron microscopy

UV/Vis: ultra-violet/visible

ACKNOWLEDGEMENTS

This work was financed by a statutory activity subsidy from the Polish Ministry of Science and Higher Education for the Faculty of Chemistry of Wroclaw University of

Science and Technology. GCD is supported by the Natural Sciences and Engineering Research Council (NSERC) of Canada through a NSERC Postdoctoral Fellowship (PDF).

DECLARATION OF INTEREST

The authors report no declarations of interest.

REFERENCES

[1] M. Rai, A. P. Ingle, S. Birla, A. Yadav, C. A. D. Santos, Strategic role of selected noble metal nanoparticles in medicine, Crit. Rev. Microbiol. 19 (2015) 1-24.

[2] P. Murawala, A. Tirmale, A. Shiras, B. L. V. Prasad, In situ synthesized BSA capped gold nanoparticles: Effective carrier of anticancer drug Methotrexate to MCF-7 breast cancer cells, Mater. Sci. Eng. C 34 (2014) 158-167.

[3] B. Saha, J. Bhattacharya, A. Mukherjee, A. Ghosh, C. Santra, A. K. Dasgupta, P. Karmakar, In vitro structural and functional evaluation of gold nanoparticles conjugated antibiotics, Nanoscale Res. Lett. 212 (2007) 614-622.

[4] E. C. Dreaden, A. M. Alkilany, X. Huang, C. J. Murphy, M. A. El-Sayed, The golden age: gold nanoparticles for biomedicine, Chem. Soc. Rev. 41 (2012) 2740-2779.

[5] I. H. El-Sayed, X. Huang, M. A. El-Sayed, Selective laser photo-thermal therapy of epithelial carcinoma using anti-EGFR antibody conjugated gold nanoparticles, Cancer Lett. 239 (2006) 129-135.

[6] A. J. Mieszawska, W. J. Mulder, Z. A. Fayad, D. P. Cormode, Multifunctional gold nanoparticles for diagnosis and therapy of disease, Mol. Pharm. 10 (2013) 831-847.

[7] L. Dykman, N. Khlebtsov, Gold nanoparticles in biomedical applications: recent advances and perspectives, Chem. Soc. Rev. 41 (2012) 2256-2282.

[8] V. Kumar, S. K. Yadav, Plant-mediated synthesis of silver and gold nanoparticles and their applications, J. Chem. Technol. Biot. 84 (2009) 151-157.

[9] S. Zeng, K. T. Yong, I. Roy, X. Q. Dinh, X. Yu, F. Luan, A review on functionalized gold nanoparticles for biosensing applications, Plasmonics 6 (2011) 491-506.

[10] P. L. Gkizis, M. Stratakis, I. N. Lykakis, Catalytic activation of hydrazine hydrate by gold nanoparticles: Chemoselective reduction of nitro compounds into amines, Catal. Commun. 36 (2013) 48-51.

[11] A. S. K. Hashmi, G. J. Hutchings, Gold catalysis, Angew. Chem. Int. Ed. 45 (2006) 7896-7936.

[12] L. Mokoena, G. Pattrick, M. S. Scurrell, Catalytic activity of gold-perovskite catalysts in the oxidation of carbon monoxide, Gold. Bull. 49 (2016) 53-61.

[13] S. Carrettin, M. C. Blanco, A. Corma, A. S. K. Hashmi, Heterogeneous gold-catalysed synthesis of phenols, Adv. Synth. Catal. 348 (2006) 1283-1288.

[14] A. S. K. Hashmi, M. C. Blanco, D. Fischer, J. W. Bats, Gold catalysis: evidence for the in-situ reduction of gold(III) during the cyclization of allenyl carbinols, Eur. J. Org. Chem. 1 (2006) 1387-1389.

[15] J. Santhoshkumar, S. Rajeshkuman, S. Venkat Kumar, Phyto-assisted synthesis, characterization, and applications of gold nanoparticles – a review, Biochem. Biophys. Rep. 11 (2017) 46-57.

[16] A. Dzimitrowicz, P. Jamroz, G. diCenzo, I. Sergiel, T. Kozlecki, P. Pohl, Preparation and characterization of gold nanoparticles prepared with aqueous extracts of *Lamiaceae* plants and the effect of follow-up treatment with atmospheric pressure glow discharge, Arab. J. Chem. (2016a) DOI: 10.1016/j.arabjc.2016.04.004.

[17] A. Dzimitrowicz, S. Berent, A. Motyka, P. Jamroz, K. Kurcbach, W. Sledz, P. Pohl, Comparison of the characteristics of gold nanoparticles synthesized using aqueous plant extracts and natural plant essentials oils, Arab. J. Chem. (2016b) DOI: 10.2016/j.arabc.2016.09.007.

[18] K. Gopinath, K. S. Venkatesh, R. Ilangovan, K. Sankaranarayanan, A. Arumugam, Green synthesis of gold nanoparticles from leaf extract of *Terminalia arjuna*, for the enhanced mitotic cell division and pollen germination activity, Ind. Crops Prod. 50 (2013) 737-742.

[19] A. Muthuvel, K. Adavallan, K. Balamurugan, N. Krishnakumar, Biosynthesis of gold nanoparticles using *Solanum nigrum* leaf extract and screening their free radical scavenging and antibacterial properties, Biomed. Prevent. Nutr. 42 (2014) 325-332.

[20] P. Priya Tharishini, N. C. Saraswathy, K. H. Smila, D. Yuvaraj, M. Chandran, P. Vivek, Green synthesis of gold nano particles from Cassia auriculata leaf aqueous extract and its cytotoxicity effect on in vitro cell line, Int. J. Chemtech. Res. 6 (2014) 4241-4250.

[21] M. N. Nadagouda, N. Iyanna, J. Lalley, C. Han, D. D. Dionysiou, R. S.Varma, Synthesis of silver and gold nan oparticles using antioxidants from blackberry, blueberry, pomegranate, and turmeric extracts, ACS Sustain. Chem. Eng. 27 (2014) 1717-1723.

[22] N. Muniyappan, N. S. J. Nagarajan, Green synthesis of gold nanoparticles using *Curcuma pseudomontana* essential oil its biological activity and cytotoxicity against Human ductal breast carcinoma cells T47D, J. Environ. Chem. Eng. 2 (2014) 2037-2044.

[23] D. Philip, Honey mediated green synthesis of gold nanoparticles, Spectrochim Acta A Mol. Biomol. Spectrosc. 73 (2009) 650-653.

[24] C. C. Wu, D. W. Chen, A facile and completely green route for synthesizing gold nanoparticles by the use of drink additives, Gold Bull. 40 (2007) 206-212.

[25] S. S. Dash, B. G. Bag, Synthesis of gold nanoparticles using renewable *Punica granatum* juice and study of its catalytic activity, Appl. Nanosci. 4 (2014) 55-59.

[26] P. This, T. Lacombe, M. R. Thomas, Historical origins and genetic diversity of wine grapes, Trends in Genet. 22 (2006) 511-519.

[27] E. I. Geana, A. Marinescu, A. M. Iordache, C. Sandru, R. E. Ionete, C. Bala, Differentiation of Romanian wines on geographical origin and wine variety by elemental composition and phenolic components, Food Anal. Methods, 7 (2014) 2064-2074.

[28] M. O. Downey, N. K. Dokoozlian, M. P. Krstic, Cultural practice and environmental impacts on the flavonoid composition of grapes and wine: a review of recent research, Am. J. Enol. Vitic. 57 (2006) 257-268.

[29] A. L. Waterhouse, Wine phenolics, Ann. N. Y. Acad. Sci. 957 (2002) 21-36.

[30] N. Balasundram, K. Sundram, S. Samman, Phenolic compounds in plants and agri-industrial by-products: antioxidant activity, occurrence, and potential uses, Food Chem. 99 (2006) 191-203.

[31] G. A. Agbor, J. AVinson, P. E. Donnelly, Folin-Ciocalteu reagent for polyphenolic assay, Int. J. Food. Sci. Nutr. 3 (2014) 147-156.

[32] C. S. Chidan Kumar, R. Mythily, R. Venkatachalapathy, S. Chandraju, Bio-mimic conversion of Maida (polysaccharides) to reducing sugars by acid hydrolysis and its estimation using standard methods, Int. Food Res. J. 21 (2014) 523-526.

[33] J. R. Navarro, M. H. Werts, Resonant light scattering spectroscopy of gold, silver and gold-silver alloy nanoparticles and optical detection in microfluidic channels, Analyst. 138 (2013) 583-592.

[34] C. Matzler (2002). MATLAB functions for Mie scattering and absorption. Research report, University of Bern [Online]. Available at: http://citeseerx.ist.psu.edu/viewdoc/download?doi=10.1.1.586.2635&rep=rep1&type=pdf.

[35] A. Dzimitrowicz, P. Jamroz, K. Greda, P. Nowak, M. Nyk, P. Pohl, The influence of stabilizers on the production of gold nanoparticles by direct current atmospheric pressure glow microdischarge generated in contact with liquid flowing cathode, J. Nanopart. Res. 17 (2015) 185.

[36] M. Alsawafta, S. Badilescu, A. Paneri, V. V. Truong, M. Packirisamy, Gold-Poly (methyl methacrylate) nanocomposite films for plasmonic biosensing applications, Polymers 3 (2011) 1833-1848.

[37] X. Huang, M. A. El-Sayed, Gold nanoparticles: optical properties and implementations in cancer diagnosis and photothermal therapy, J. Adv. Res. 1 (2010) 13-28

[38] E. Hao, G. C. Schatz, Electromagnetic fields around silver nanoparticles and dimmers, J. Phys. Chem. 120 (2014) 357-366.

[39] P. K. Jain, K. S. Lee, I. H. El-Sayed, M. A. El-Sayed, Calculated absorption and scattering properties of gold nanoparticles of different size, shape, and composition: applications in biological imaging and biomedicine, J. Phys. Chem. B. 110 (2006) 7238-7248.

[40] I. H. El-Sayed, X. Huang, M. A. El-Sayed. Selective laser photo-thermal therapy of epithelial carcinoma using anti-EGFR antibody conjugated gold nanoparticles, Cancer Lett. 239 (2006) 129-135.

[41] S. Hong, X. Li, Optimal size of gold nanoparticles for surface-enhanced raman spectroscopy under different conditions, J. Nanomater. 2013 (2013) 790323.

[42] N. Shah, W. Cynkar, P. Smith, D. Cozzolino, Use of attenuated total reflectance midinfrared for rapid and real-time analysis of compositional parameters in commercial white grape juice, J. Agric. Food Chem. 58 (2010) 3279-3283.

[43] D. Murphy, M. N. de Pinho, An ATR-FTIR study of water in cellulose acetate membranes prepared by phase inversion, J. Membr. Sci. Technol. 106 (1995) 245-257.

[44] C. Bevin, A. Ferguson, W. Perry, L. Janik, D. Cozollino, Development of a rapid ‘‘fingerprinting” system for wine authenticity by mid-infrared spectroscopy, J. Agric. Food Chem. 54 (2006) 9713-9718.

[45] A. H. Lu, E. L. Salabas, F. Schuth, Magnetic nanoparticles: synthesis, protection, functionalization, and application. Angew. Chem. Int. Ed. 46 (2007) 1222-1244.

[46] R. A. Cocciardi, A. A. Ismail, J. Sedman, Investigation of the potential utility of single-bounce attenuated total reflectance Fourier transform infrared spectroscopy in the analysis of distilled liquors and wines, J. Agric. Food Chem. 53 (2005) 2803-2809.

[47] L. Saavedra, C. Barbas, Validated capillary electrophoresis method for small-anions measurement in wines, Electrophoresis 24 (2003) 2235-2243.

[48] G. D. Manrique, F. M. Lajolo, FT-IR spectroscopy as a tool for measuring degree of methyl esterification in pectins isolated from ripening papaya fruit, Postharvest Biol. Technol. 25 (2002) 99-107.

[49] A. Edelmann, J. Diewok, K. C. Schuster, B. Lendl, Rapid method for the discrimination of red wine cultivars based on mid infrared spectroscopy of phenolic wine extracts, J. Agric. Food Chem. 49 (2011) 1139-1145.

[50] P. A. Tarantilis, V. E. Troianou, C. S. Pappas, Y. S. Kotseridis, M. G. Polissiou, Differentiation of Greek red wines on the basis of grape variety using attenuated total reflectance Fourier transform infrared spectroscopy, Food Chem. 111 (2008) 192-196.

[51] G. J. Soleas, D. M. Goldberg, Analysis of antioxidant wine polyphenols by gas chromatography–mass spectrometry, Methods in Enzymol. 299 (1999) 137-151.

[52] J. L. Moreira, L. Santos, Spectroscopic interferences in Fouries transform infrared wine analysis, Anal. Chim. Acta. 513 (2004) 263-268.

[53] B. Stuart, Biological Applications of Infrared Spectroscopy, John Wiley and Sons, New Jersey.

[54] K. Ilaslan, I. H. Boyaci, A. Topcu, Rapid analysis of glucose, fructose and sucrose contents of commercial soft drinks using Raman spectroscopy, Food Control 48 (2015) 56-61.

[55] C. Zhu, S., Guo, Y. Fang, S. Dong, Reducing sugar: new functional molecules for the green synthesis of graphene nanosheets, ACS Nano. 4 (2010) 2429-2437.

[56] N. Ahmad, S. Sharma, M. K. Alam, V. N. Singh, S. F. Shamsi, B. R. Mehta, A. Fatma, Rapid synthesis of silver nanoparticles using dried medicinal plant of basil, Colloids Surf. B: Biointerfaces 81 (2010) 81-86.

[57] D. Philip, Green synthesis of gold and silver nanoparticles using *Hibiscus rosa* sinensis, Physica E Low Dimens. Syst. Nanostruct. 42 (2010) 1417-1424.

[58] M. Kargar, M. Reza, M. Shafiee, M. Ghashang, Green protocol preparation of ZnO nanoparticles in prunus cerasus juice media, Nanosci. Nanotechnol. Asia 5 (2015) 44-49.

FIGURE LEGENDS

Figure 1. UV/Vis absorption spectra of the colloidal AuNPs suspensions formed by incubation of Solutions I to IV with the Au(III) ions.

Figure 2. Effect of the concentration of the Au(III) ions on the absorbance of the λ_{max} of the LSPR band. The absorbance of the λ_{max} of the LSPR band, as determined by UV/Vis absorption spectroscopy, of the colloidal AuNPs suspensions formed by incubation of Solutions I to IV with three concentrations of the Au(III) ions is shown.

Figure 3. TEM images of AuNPs synthesized with Solution I (A-C), Solution II (E-G), Solution III (I-K), and Solution IV (M-O). EDX spectra of AuNPs synthesized with Solution I (D), Solution II (H), Solution III (L), and Solution IV (P).

Figure 4. Size distribution of AuNPs synthesized with Solution I (A), Solution II (B), Solution III (C) and Solution IV (D).

Figure 5. Predicted Mie extinction, absorption, and scattering efficiencies based on average size of AuNPs synthesized with Solution I and Solution II.

Figure 6. ATR FT-IR spectra of all solutions used for the synthesis of AuNPs.

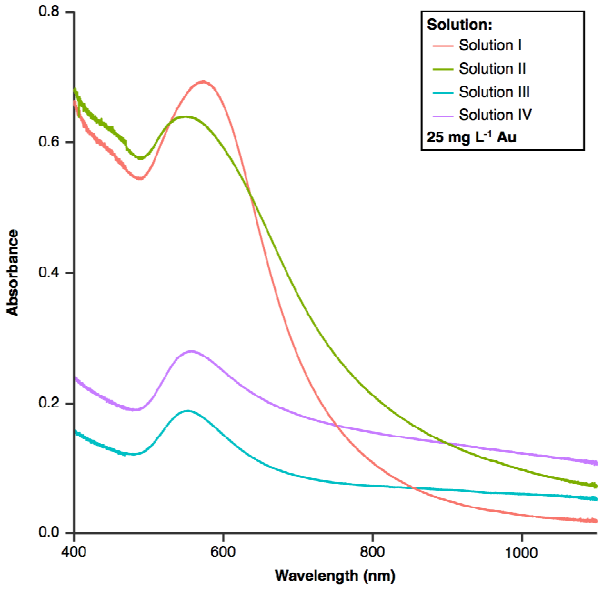

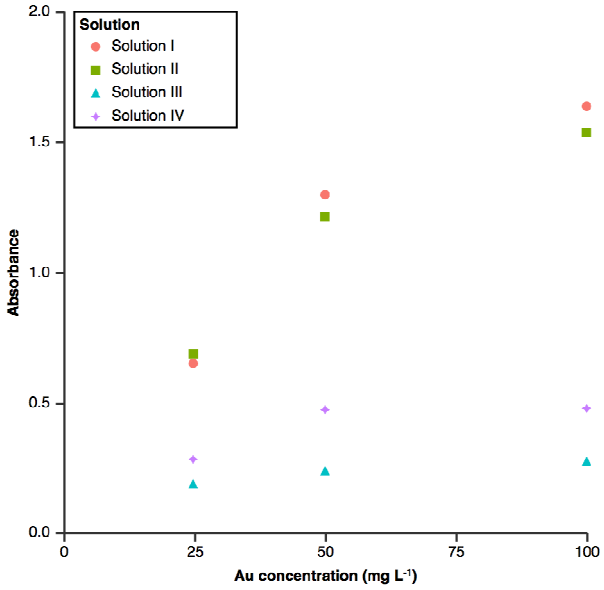

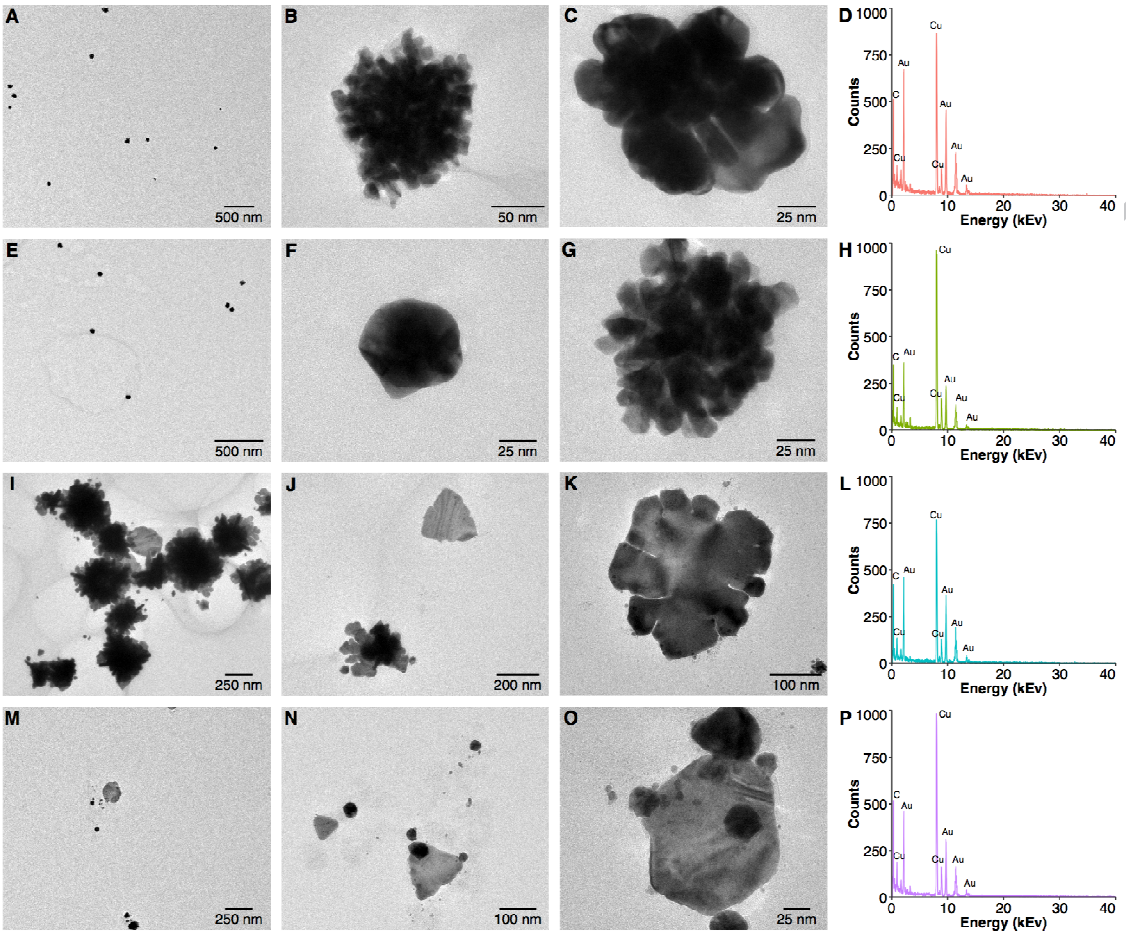

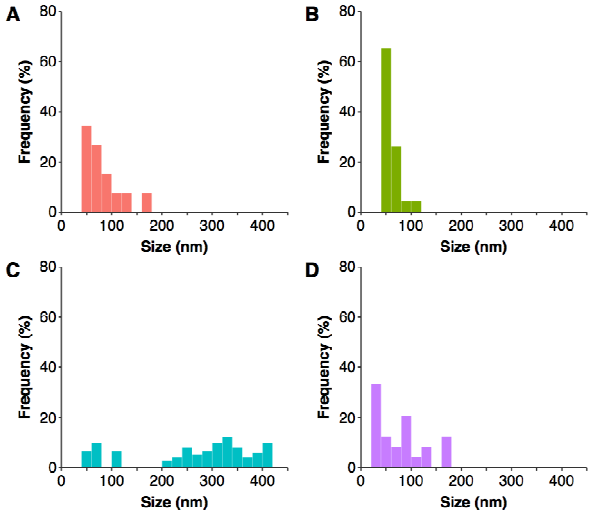

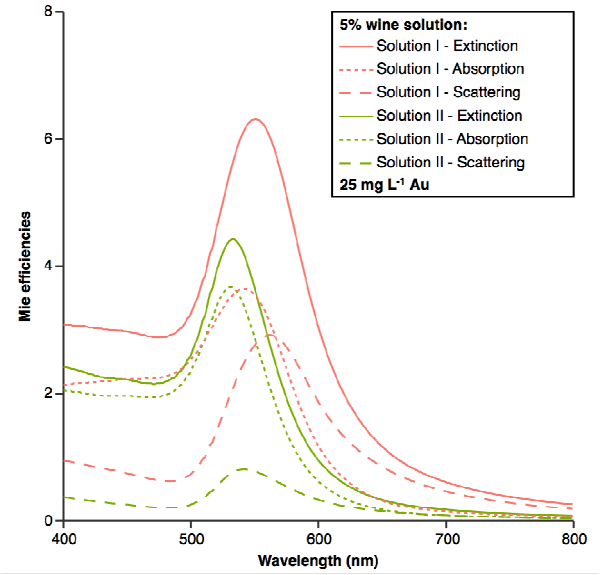

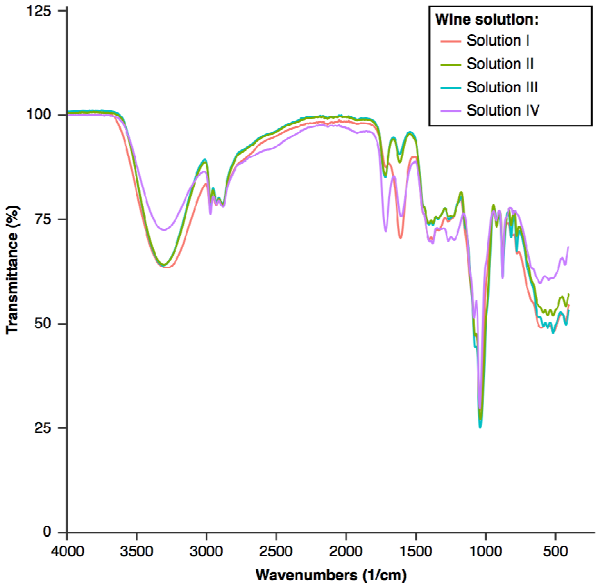

Table 1. Size (calculated based on TEM or HR-TEM measurements) of biosynthesized AuNPs

Natural product	Reducing agent	Size [nm]	References
Blackberry	fruit extract	100	[21]
Blueberry	fruit extract	200	[21]
Cassia auriculata	leaves extract	20-30	[20]
Curcuma pseudomontana	essential oil	20	[22]
Eucalyptus globules	leaves extract	12.8±6.3	[17]
Eucalyptus globules	essential oil	42.2±42.0	[17]
Honey	aqueous solution	15	[23]
Melissa officinalis	leaves extract	19.5±24.0	[16]
Mentha piperita	leaves extract	55.1±48.4	[16]
Pomegranate	fruit extract	400	[21]
Punica granatum	juice extract	23-26	[25]
Rice wine	Rice wine, Na_2CO_3	35.3±6.1	[24]
Rosmarinus officinalis	leaves extract	8.7±2.0	[17]
Rosmarinus officinalis	essential oil	60.7±60.6	[17]
Salvia officinalis	leaves extract	15.1±10.2	[16]
Solanum nigrum	leaves extract	32.0±6.0	[19]
Terminalia arjuna	leaves extract	20-50	[18]
Turmeric	fruit extract	5-60	[21]

Table 2. The total concentration of phenolic compounds (in GAE mg per L) determined in the solutions used for AuNPs biosynthesis, before and after addition of the Au(III) ions

	Red grape varieties		White grape varieties	
	Semi-sweet	Semi-dry	Semi-sweet	Dry
0 mg L^{-1} Au(III)	844	748	145	25.6
25 mg L^{-1} Au(III)	120	148	30.4	1.58

Average values (n=3)

Table 3. The total concentration of reducing sugars (in mg per L) determined in the solutions used for AuNPs biosynthesis, before and after addition of the Au(III) ions

	Red grape varieties		White grape varieties	
	Semi-sweet	Semi-dry	Semi-sweet	Dry
0 mg L^{-1} Au(III)	552	1040	1430	250
25 mg L^{-1} Au(III)	178	250	196	58.0

Average values (n=3)